Journal of Physiology (1992), **448**, *pp.* 257–274
With 7 figures
Printed in Great Britain

CYCLIC GMP-ACTIVATED CHANNELS OF SALAMANDER RETINAL RODS: SPATIAL DISTRIBUTION AND VARIATION OF RESPONSIVENESS

BY J. W. KARPEN*, D. A. LONEY AND D. A. BAYLOR

From the Neurobiology Department, Sherman Fairchild Science Center, Stanford University School of Medicine, Stanford, CA 94305, USA

(*Received 30 October 1990*)

SUMMARY

1. Patch-clamp methods were used to investigate the areal density and spatial location of cyclic GMP-activated channels in the surface membrane of salamander rod outer segments.

2. The density of active channels (i.e. channels able to respond to cyclic GMP) in patches excised from outer segments was determined from the number of active channels, N, and the membrane area, A. N was estimated from the current induced by a saturating concentration of cyclic GMP, while A was estimated from the electrical capacitance of the patch.

3. In patches excised from forty-one isolated outer segments prepared in the light the active channel density varied over a remarkable range: 0·34–629 μm^{-2}, with a mean of 166 μm^{-2}. Density was not correlated with patch area in this or any of the conditions studied.

4. The spatial distribution of open channels on the outer segment of a transducing rod was measured by recording the local dark current at various positions with a loose-patch electrode. The apparent density of open channels varied by only about $\pm 50\%$ around the circumference of the outer segment and up and down its length. This indicates that the wide range of densities in excised patches did not result from sampling a non-uniform spatial distribution of channels.

5. Patches excised from sixteen dark-adapted whole cells with healthy appearances and saturating light responses of normal size had active channel densities of 1·1–200 μm^{-2}, with a mean of 60 μm^{-2}. Patches from twenty light-adapted whole cells had similar densities. Many densities from the whole cells were much lower than expected. This, and the wide variation in densities, suggests that obtaining a patch often lowered the density of active channels. The number of channels in a patch was quite stable from 1 s to 30 min after excision, ruling out progressive denaturation or adsorption of channels to the glass as a cause for this effect.

6. The mean active channel density in patches excised from whole cells was lower with calcium present in the external solution than with calcium absent (80 *vs.* 152 μm^{-2}, $n = 36$ and 30 respectively).

* Present address: Department of Physiology, Campus Box C240, University of Colorado School of Medicine, 4200 East Ninth Avenue, Denver, CO 80262, USA.

MS 8894

7. We conclude that copies of the channel protein were present at a density of at least 650 μm^{-2} in the surface membrane of the outer segment and that the distribution of channels was fairly uniform on a 1 μm scale. The process that lowers the active channel density in excised patches may depend upon a physical artifact of patch excision and/or a Ca^{2+}-dependent enzymatic mechanism.

INTRODUCTION

There is general agreement that the transmitter cyclic GMP controls the ionic channels that generate the electrical response to light in retinal rods (reviewed in McNaughton, 1990). In the dark cyclic GMP binds to channels and holds them open, allowing cations to enter the outer segment. Light lowers the internal concentration of cyclic GMP, closing the channels, blocking the inward current, and hyperpolarizing the cell.

Several lines of evidence indicate that the cyclic GMP-activated channel is present in the surface membrane of the outer segment but not in the disc membranes (Bauer, 1988; Cook, Molday, Reid, Kaupp & Molday, 1989; Caretta & Saibil, 1989). Only a few channels seem to be present in the inner segment (Watanabe & Matthews, 1988). Little information is available, however, on the density and spatial distribution of channels within the outer segment's surface membrane. Biochemical estimates of channel density are subject to errors in determining the amount of protein present as well as uncertainty about the number of subunits that form the channel. Furthermore, since the channel may be enzymatically regulated, it is important to know the density of channels that are active, i.e. able to respond to cyclic GMP. Noise analysis (Gray & Attwell, 1985; Bodoia & Detwiler, 1985) gives estimates for the number of channels that are open in darkness, but open channels comprise only a small fraction of the total number of active channels (reviewed in Yau & Baylor, 1989). It is also not clear whether channels are present at uniform density on the outer segment or are instead arranged in an ordered spatial pattern.

We describe experiments to determine the density of active channels and their spatial distribution on the outer segment. Unexpectedly, we found that the density of channels in excised patches varies widely and that excising a patch may lower the number of channels available to respond to cyclic GMP. Abstracts describing portions of the work have already appeared (Loney, Karpen & Baylor, 1989; Karpen, Loney & Baylor, 1990).

METHODS

Preparation

Experiments were performed on retinal rods from larval tiger salamanders, *Ambystoma tigrinum*, maintained as described in Baylor & Nunn (1986). After rapid decapitation the brain and spinal cord were pithed and the eyes removed. The eyes were hemisected, and the retinas were isolated into Ringer I or II solutions (see composition in Table 1). Pieces of isolated retina were kept refrigerated in Ringer solution for up to 12 h before use. Small pieces of isolated retina were placed in an experimental chamber modified from that described by Baylor, Lamb & Yau (1979). In the chamber, which had a fluid volume of about 100 μl, the pieces of retina were teased with fine bent needles, producing isolated rods and isolated outer segments. When patches were to be excised from isolated outer segments, the floor of the chamber was made sticky by pre-coating it with poly-L-

lysine. The chamber was filled with 1 mg ml^{-1} poly-L-lysine hydrobromide (rel. mol. mass 30000–70000 Sigma) for 2 min followed by thorough rinsing. The outer segments adhered to the floor, preventing them from rolling away when the patch electrode approached. For patch excision or loose-patch recording from intact isolated rods, the floor was not coated; instead the cell was held by drawing part of its inner segment into a suction electrode. For dark adaptation an animal

TABLE 1. Composition of solutions

Solution	NaCl	KCl	$CaCl_2$	$MgCl_2$	D-Glucose	HEPES	Tris	EDTA	EGTA	Cyclic GMP
Ringer I	111	2·5	1·5	6·0	10	3	0	0·02	0	0
Ringer II	111	2·5	1·0	1·0	10	3	0	0·02	0	0
Sodium, zero divalents	130	0	0	0	0	0	2	0·02–0·1	0	0 or 0·5
Ringer, zero divalents	111	2·5	0	0	10	3	0	4	0	0
Zero-Ca^{2+} Ringer I	111	2·5	0	6·0	10	3	0	0·02	0·3	0
Zero-Ca^{2+} Ringer II	111	2·5	0	1·0	10	3	0	0·02	0·3	0
Excising solution I	130	0	0·210	0·1	0	0	2	0	0·2	0·5
Excising solution II	130	0	0	0·1	0	0	2	0	0·2	0·5

All concentrations are mM. All solutions were pH 7·6. In excising solution I, calculated concentration of free Ca^{2+}, 0·010 mM.

was kept in aerated water in a light-tight container for at least 2 h. Enucleation was performed under dim red light and subsequent procedures were carried out under infra-red light, with the aid of infra-red/visible image converters (Baylor *et al.* 1979) and an infra-red video viewing system attached to the inverted microscope. A gravity-driven perfusion system allowed the solution in the experimental chamber to be changed within about 20 s.

Solutions

The composition of solutions is listed in Table 1. A concentration of 6 mM-Mg^{2+} was used in some of the solutions in initial attempts to improve seal formation by the patch pipette (see Baylor & Nunn, 1986), but as this strategy seemed to have little effect 1 mM was used in later experiments.

Electrodes

Silane-treated borosilicate suction electrodes with orifices 7·5 μm in diameter were used for holding cells and recording whole-cell photocurrents. The suction electrodes were filled with Ringer solution (see Table 1). Patch pipettes were made from borosilicate glass. After pulling, a miniature O_2–H_2 torch was used to make a right-angle bend in the shank. The bend allowed the tip of the electrode to be located precisely in the horizontal plane as the electrode was lowered. Pipettes for membrane excision had orifices about 1 μm in diameter and resistances near 3 MΩ. They were Sylgard coated to reduce stray capacitance, lightly fire-polished, and filled with sodium, zero divalent solution (Table 1). Pipettes for loose-patch recording had slightly larger tips (6 μm o.d., 2·5 μm i.d. or 4 μm o.d., 0·65 μm i.d.) and after fire-polishing were treated with silane to prevent seal formation. They were filled with zero divalent Ringer solution (Table 1). This solution scaled up the local dark current, mainly by reducing divalent block of the channels (see Yau & Baylor, 1989). A high concentration of EDTA, 4 mM, was used to hold the divalent cation concentration very low during recording, even though divalents entered the tip from the bulk solution through the leakage conductance.

Recording

Patch currents were recorded with an Axopatch 1A amplifier (Axon Instruments). Currents from excised patches were low-pass filtered (8-pole Bessel, −3 dB frequency 4 kHz), sampled at 100 kHz and stored and analysed with a PDP 11/73 computer (Indec Systems). Loose-patch currents were low-pass filtered at 10 Hz. Whole-cell currents from the suction electrode were recorded with a Dagan 8900 patch-clamp amplifier. Loose-patch and whole-cell currents were stored with a PCM videotape system (Neuro-Corder DR-484, Neuro Data Instrument Corp.). Video images from experiments on whole cells were also stored on a video recorder.

Channel density measurement

Unless otherwise noted, patches were excised while the whole cell or the isolated outer segment was bathed in Ringer I or II solution (Table 1). Typically the seal resistances of the patches were between 1 and 30 GΩ. The density of active channels in an excised patch was determined as follows (see Fig. 1). The number of active channels in the patch, N, was estimated from the difference in the ionic currents evoked by +50 mV pulses in the presence and absence of a saturating concentration of cyclic GMP (500 μM) in sodium, zero divalent solution (Table 1) on the cytoplasmic side of the patch. The zero divalent solution scaled up the cyclic GMP-induced currents by eliminating channel block by divalent cations. N was obtained by dividing the difference current by 1·2 pA, the estimated mean current through a single channel at saturating cyclic GMP. This value, upon which the absolute channel density estimates directly depend, was obtained in the following way. Matthews and Watanabe's records from a single channel at 1 mM-cyclic GMP in symmetrical low divalent solutions (1988, Fig. 4) show a mean current of −1·2 pA at a voltage of −71 mV. To estimate the mean current expected at +50 mV, the voltage used here, allowance must be made for the moderate outward rectification in the macroscopic currents through the channels under these conditions (e.g. Yau, Haynes & Nakatani, 1986). Allowing for the rectification, a current near +1·2 pA is expected at +50 mV. This mean current amplitude is also consistent with the mean conductance during the fast, large amplitude bursts observed in previous single-channel recordings at low cyclic GMP (Haynes, Kay & Yau, 1986; Zimmerman & Baylor, 1986). We suppose that the value of 1·2 pA could be in error by up to about ±30%.

For patches with large cyclic GMP-activated currents the voltage drop in the pipette series resistance reduced the 50 mV command voltage across the patch. When necessary the recorded current i was corrected to the size expected without the series resistance error, using the relation $i' = iV/(V - iR_p)$, where i' is the corrected current, V is the command potential, and R_p is the measured pipette resistance. Strictly this correction applies only when the current–voltage relation is linear. The deviation from linearity is small between 0 and +50 mV, however, and at worst the linear correction should have underestimated the current by only about 6%.

The patch area, A, was determined from its capacitance, using a modification of the method of Sakmann & Neher (1983). With the tip of the patch pipette just above a cured Sylgard bead on the bottom of the chamber, the currents evoked by a +50 mV pulse were recorded in sodium, zero divalent solution without cyclic GMP.

The pipette was then lowered onto the bead, which blocked the membrane capacitance but left the electrode and stray capacitance unchanged. The pipette was lowered until the steady component of the leakage current decreased by about an order of magnitude; the large resistance placed in series with the tip effectively eliminated rapid charging of the membrane capacitance even if the membrane had not broken (see below). Care was taken to avoid two sources of artifact: (1) the control recording was made with the tip only about 10 μm above the surface of the Sylgard bead, so that when the electrode was lowered the length immersed in the bathing solution did not change, causing spurious changes in capacitance, (2) puncturing the bead was avoided, so that none of the electrode shaft was occluded. The reproducibility of the measurements indicated that these artifacts were successfully avoided (see Results). With the tip of the electrode blocked, currents evoked by the 50 mV pulse were again recorded and the difference currents calculated. The capacitive component of the difference current was obtained by the method discussed on p. 262. The capacitive current, $i_c(t)$, was then used to calculate the membrane area, A, using the relation

$$A = \frac{\int i_c(t)\,dt}{C\Delta V}, \tag{1}$$

in which ΔV is the applied voltage step and C is the specific membrane capacitance, which was taken as 1 μF cm^{-2}. Specific capacitances near this have been found for membranes of a variety of cells (e.g. Hille, 1984, pp. 25–26), and a similar value (0·8 μF cm^{-2}) was obtained for the surface membrane of frog rod outer segments by analysing the AC admittance of outer segment suspensions (Falk & Fatt, 1968). The absolute channel densities derived here depend directly on the assumed value of C. Usually contact with the Sylgard broke the patch, but sometimes it did not, allowing the membrane area to be remeasured.

Some patches, 34 of 205 analysed, responded to cyclic GMP only after the tip of the pipette was touched to Sylgard resin, apparently rupturing a vesicle which blocked the inner surface of the patch membrane. Forty-six of the 205 patches did not respond to cyclic GMP and broke on contact with Sylgard. It is not clear whether these 'refractory' patches were vesicles or simply patches that contained no cyclic GMP-activated channels; these patches were excluded from the analysis. Even if all the refractory patches lacked channels the conclusions would not be seriously altered. Furthermore, since excision did sometimes produce vesicles, it seems likely that some of the refractory patches were vesicles which broke completely on contact with Sylgard.

Loose-patch recordings of local dark current density

The inner segment of a dark-adapted cell was drawn partly into a suction electrode (see Fig. 4). The cell was lowered and the outer segment placed in a shallow linear groove scribed in the floor of the experimental chamber with a diamond marking pen. The groove prevented the outer segment from rolling when the loose patch electrode was pressed against it. Positive pressure was briefly put on the electrode to expel divalent cations from its tip and then, with the pressure neutral, the electrode was pressed on the outer segment until the resistance rose by roughly a factor of 2. A saturating flash from an optical stimulator (Baylor *et al.* 1979) was delivered while recording the whole-cell current with the suction electrode and the local current with the loose-patch electrode. Recordings were made around the circumference of the rod by raising the cell, rotating it on its long axis by turning the suction electrode with a specially constructed electrode holder, and relowering it to the floor. Rotation through angles up to 360 deg was accomplished by manually turning a flexible cable attached to the holder. The loose-patch electrode was also placed at various longitudinal positions on the outer segment. The patch pipette dimpled the outer segment relatively little and left it in good condition after many measurements. Photocurrents, p, recorded by the loose-patch electrode were corrected for inefficiency in current collection with the expression $p' = pg_o(g_o - g_f)^{-1}$, where p' is the corrected current and g_o and g_f are the respective pipette conductances measured before and after pressing the electrode on the cell. The true whole-cell photocurrent was estimated from the recorded whole-cell current, assuming that the fraction of current recorded by the suction electrode was proportional to the fraction of the inner segment area within the electrode and that the collection efficiency was 80 %.

The interpretation of local current distributions determined by loose-patch recording depends upon how the low divalent solution in the pipette is assumed to perturb the cell. If the electrode scaled up the local current solely by relieving divalent block of channels, the channels' open probability would presumably be similar at all positions, and the size of the local current would reflect the local density of active channels. If instead the loose-patch electrode perturbed the internal concentrations of Ca^{2+} and cyclic GMP, and if these effects varied with the local density of active channels, apparent variations in channel density would be accentuated. Thus, in a region of higher channel density, the loose-patch pipette would cause a larger drop in internal Ca^{2+}, a larger rise in cyclic GMP concentration (reviewed in McNaughton, 1990), and a larger increase in the open probability.

Apparently the loose-patch pipette had little global effect on the outer segment, for removing the pipette lowered the whole-cell current by roughly the amount expected for removing the intense local current at the tip of the patch pipette. For example, in one trial on the cell of Fig. 4 the measured whole-cell currents were 13·0 and 10·5 pA before and after the loose-patch pipette was removed. The 2·5 pA decrease in the whole-cell current, corrected for the fraction of current recorded, gave the true decrease as 15·6 pA, which is comparable to the corrected loose-patch current of 13·5 pA.

The amount by which the low concentration of divalent cations in the loose-patch pipette scaled up the local dark current can be estimated in the following way. For the cell of Fig. 4 the dark current was estimated as 40·5 pA in the absence of the loose-patch pipette. Assuming that the outer

segment's surface area was 1000 μm^2, the 4·9 μm^2 patch of membrane at the orifice of the loose-patch pipette would have had a current of $(40·5/1000) \times 4·9 = 0·20$ pA with normal external divalents. The corrected loose-patch current of 13·5 pA implies that removal of external divalents scaled up the local current by a factor of $13·5/0·20 = 67·5$.

RESULTS

Number of active channels and membrane area of excised patches

Figure 1 illustrates how the active channel density was obtained. The upper trace in Fig. 1*A* is the current across an inside-out patch when a +50 mV pulse was applied with sodium, zero divalent solution containing 500 μM-cyclic GMP in the chamber. The middle trace is the current recorded after washing the cyclic GMP out of the chamber. The difference current, plotted in the lower trace, flowed through cyclic GMP-activated channels. The peak difference current, corrected for the small series resistance error, was divided by the assumed single-channel current of 1·2 pA, giving the number N of active channels as 428.

Figure 1*B* illustrates how the area of the membrane patch was obtained. The upper trace was recorded in sodium, zero divalent solution with the pipette just above the Sylgard bead on the floor of the chamber. The middle trace was recorded with the tip of the pipette pushed against the bead. The difference current, plotted below, is the sum of the capacitive current and the leakage current across the membrane and seal resistance. At long times the difference current is purely leak (resistive), and by scaling the step response of the recording system to fit the final level, the entire time course of the leakage component was obtained (thin line). Subtraction of the leakage component leaves the capacitive current across the membrane. For this patch, $\int i_c dt$ was 3·67 fC and the membrane capacitance was 73·4 fF. The membrane area, calculated by eqn (1), was 7·34 μm^2. The channel density, N/A, was 58·3 μm^{-2}.

Measurements on 136 patches gave the distribution of areas shown in Fig. 2, for which the mean area was 11·7 μm^2. From preliminary measurements on a smaller number of patches Loney *et al.* (1989) reported areas that ranged between 4 and 58 μm^2. At first glance the areas may seem large for pipettes with 1 μm orifices, and indeed Zimmerman & Baylor (1986) supposed that the patch area might be roughly 2 μm^2. During seal formation, however, a small 'bleb' of tissue was seen to enter the tip (see also Sakmann & Neher, 1983). The mean area of 12 μm^2 is consistent with a roughly spherical bleb about 2 μm in diameter. A bleb of this size is also consistent with the mean volume of 7·5 μm^3 obtained by analysing the kinetics of diffusion in patches from rod outer segments (Zimmerman, Karpen & Baylor, 1988). As expected, the patch areas were small when a seal formed without applying negative pressure and large when stronger negative pressure had to be applied for some time. When contact with the Sylgard did not rupture the patch the membrane area could be remeasured, and in these cases the areas were in good agreement.

Active channel density in light-adapted isolated outer segments

The upper histogram in Fig. 3 shows the distribution of active channel densities in patches excised from isolated outer segments of bleached rods. The patches were taken from outer segments that appeared healthy, with high refractive index, normal size, and straight edges. The densities varied over a remarkably wide range: 0·34–629 μm^{-2}. The mean density for the forty-one patches was 166 μm^{-2}, and the

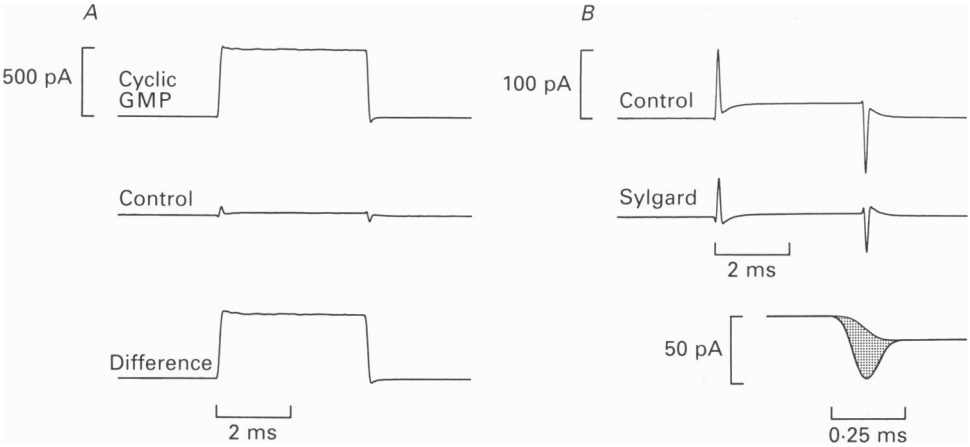

Fig. 1. Determination of density of active channels in an inside-out patch from the outer segment. *A*, number of channels. Patch currents evoked by +50 mV pulses with 500 μM-cyclic GMP-sodium, zero divalent solution (Table 1), or the same solution without cyclic GMP, in the chamber. The number of active channels was estimated from the cyclic GMP-activated difference current (see text). *B*, patch area. Currents evoked by +50 mV pulses with the patch in sodium, zero divalent solution before and after the tip of the electrode was pushed against Sylgard to block the membrane capacitance. The difference current at the end of the pulse is plotted on expanded scales below, with the leakage component indicated by the light line (see text). Shaded area is the charge that polarized the membrane capacitance. Difference currents were calculated from the average responses in eleven trials each in *A*, twenty trials each in *B*. Capacitance compensation was adjusted between recordings in *A* and *B*. Patch was excised from the outer segment of a light-adapted whole cell bathed in zero-Ca^{2+} Ringer II solution (Table 1). The pipette resistance measured before seal formation was 3·5 MΩ, and the series resistance error was 1·7 mV. Seal resistance was 2·2 GΩ. Channel density estimated as 58·3 μm^{-2}.

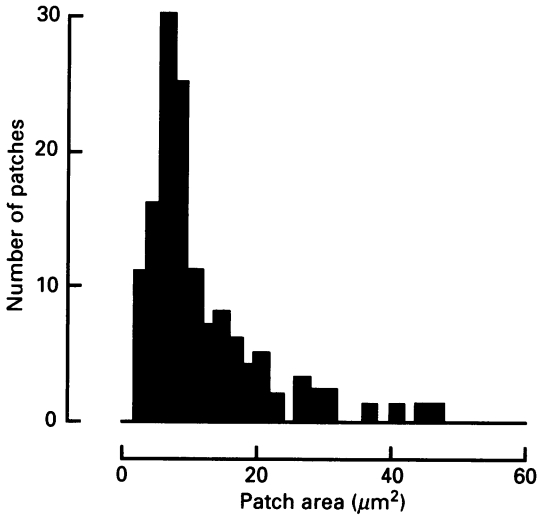

Fig. 2. Distribution of areas of 136 excised patches, determined from patch capacitance assuming a specific membrane capacitance of 1 μF cm^{-2}. Mean patch area was 11·7 μm^2, range 2·1–46·2 μm^2. Patches were excised from isolated outer segments or the outer segments of whole cells. Pipette orifices were about 1 μm in diameter.

standard deviation was 178 μm^{-2}. The mean patch area was 15·3 μm^2. There was no correlation between the area of the patch and the measured density of channels in this or any of the distributions to be presented.

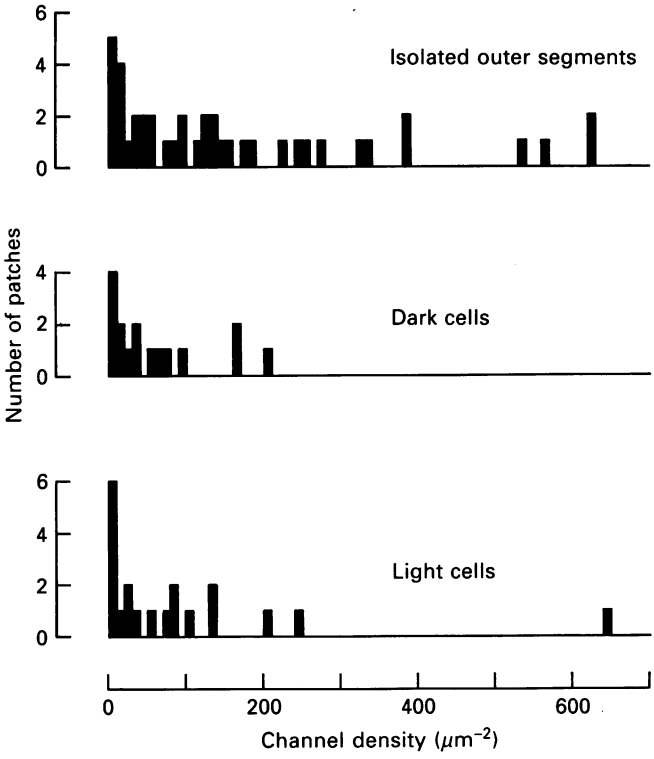

Fig. 3. Histograms of active channel densities in membrane patches excised from isolated outer segments prepared in the light ($n = 41$), outer segments of dark-adapted, transducing whole rods ($n = 16$), and outer segments of light-adapted whole rods ($n = 20$). Channel densities were, respectively (mean ± standard deviation): 166 ± 178, 60–65 and 96 ± 146 μm^{-2}. Mean patch areas were 15·3, 12·4 and 10·8 μm^2 respectively. Isolated outer segments were in Ringer I solution before patch excision, whole cells in Ringer II solution.

Although single-channel currents were not recorded in these experiments, we attribute the small size of the macroscopic currents measured in some patches to a small number of active channels rather than a small mean elementary current. This interpretation is based upon results from patches containing only a single active channel (Taylor & Baylor, 1990). In these patches, which had channel densities $< 10\ \mu m^{-2}$, the single-channel current amplitudes were similar to those described previously (Haynes *et al.* 1986; Zimmerman & Baylor, 1986; Matthews & Watanabe, 1988).

The wide range of channel densities in the top histogram of Fig. 3 cannot be explained by assuming that the electrode sampled a random spatial distribution which had the same mean density on different outer segments. If this were so, the expected number of channels in a patch would be a Poisson-distributed random variable with variance equal to the mean. Given the observed mean density of

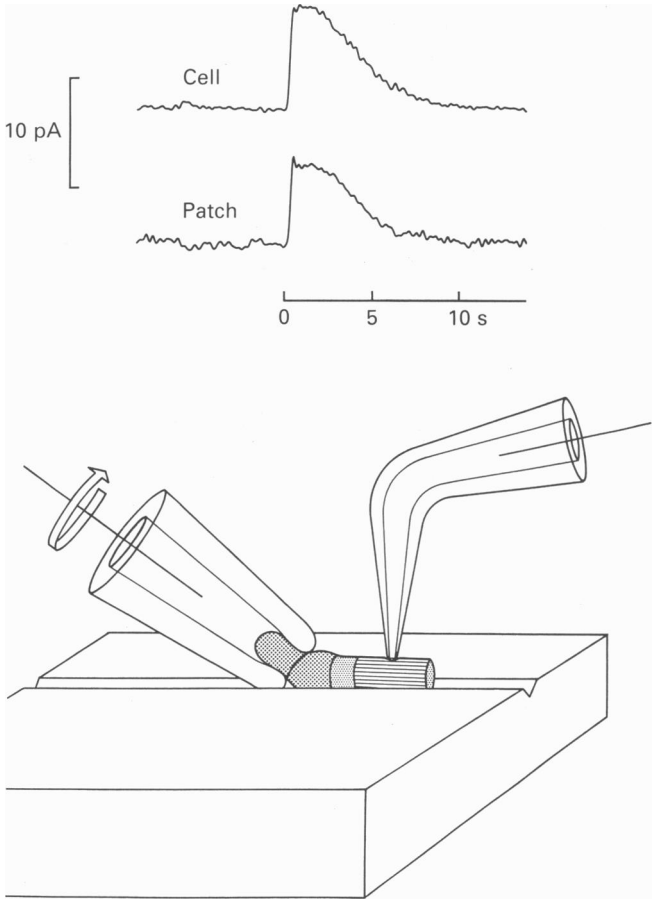

Fig. 4. Loose-patch and whole-cell recording from an intact transducing rod. The bottom diagram shows the suction electrode (left) used to hold the rod and record its whole-cell current. A loose-patch electrode (right) was pressed on the outer segment at different positions to record the local dark current. For recording at different circumferential positions the rod was rotated around its long axis. Placing the outer segment in a shallow groove in the floor of the chamber prevented it from rolling away from the loose-patch electrode. The traces above show simultaneous whole-cell and loose-patch photocurrents recorded by this method. A bright flash of light was delivered at time zero. About 0·22 of the inner segment's membrane was in the suction electrode, and assuming a collection efficiency of 0·8 the true whole-cell current was estimated as 54 pA. Loose-patch response is large because the electrode was filled with zero divalent Ringer solution (Table 1), which eliminated channel block by external divalents. The loose-patch pipette had a 2·5 μm diameter orifice, and when pressed against the cell its conductance dropped to 0·48 of the initial value. The measured loose-patch current of 7·0 pA gave a corrected value of $7/(1-0{\cdot}48) = 13{\cdot}5$ pA. Recordings from the cell plotted by open circles in Fig. 5.

166 μm^{-2} in the histogram and the patch areas, the observations should have distributed about this value with a standard deviation less than 10 μm^{-2}. The standard deviation in the experimental distribution was 178 μm^{-2}.

Spatial arrangement of open channels on the outer segment

One might explain the wide variation in measured channel density by assuming that channels are arranged in an orderly spatial pattern, so that patches may be excised from regions of high or low density. Evidence that the number of open

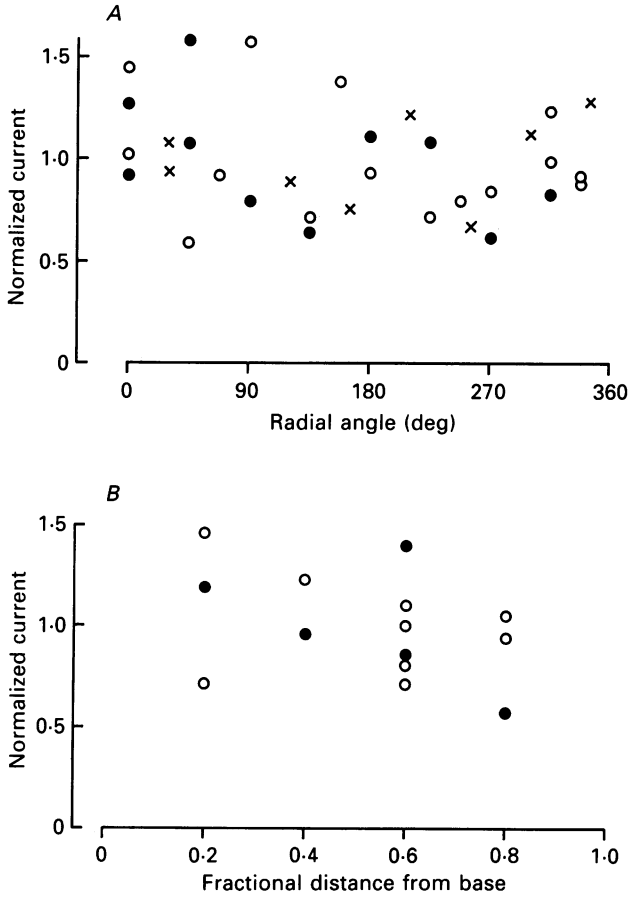

Fig. 5. Amplitude of saturating photocurrent recorded by loose-patch electrode at different positions on the outer segment. *A*, photocurrent amplitude as a function of circumferential position on three cells. Currents recorded by the loose-patch electrode were corrected for imperfect current collection (see Methods) and normalized with respect to the cell's mean current over all trials. Corrected mean currents were: ○, 16·3 pA; ●, 14·4 pA; ×, 6·4 pA. A linear decrease over time in the currents from the first cell was removed by scaling the currents with factors determined by linear regression analysis on all the points. *B*, photocurrent amplitude as a function of longitudinal position. Results from two of the cells illustrated in *A*, plotted by the same symbols. Currents were corrected and scaled as described for part *A*. Electrode orifice 2·5 μm diameter for *A* and *B*.

channels per unit length of the outer segment is approximately constant (Baylor *et al.* 1979) does not rule out a non-uniform circumferential arrangement such as a longitudinal 'stripe' of channels attached to the axoneme.

The spatial distribution of open channels was examined by using a loose-patch electrode to record the response to a saturating flash at various positions on the outer

segment of an intact transducing rod (see Fig. 4). A pivot on the electrode holder allowed the cell to be rotated on its long axis so that recordings could be made at any circumferential position. Measurements were also made at various longitudinal positions. Since a bright flash completely shuts off the dark current (Penn & Hagins, 1972; Baylor *et al.* 1979), the amplitude of the saturating response recorded by the loose-patch electrode will be proportional to the number of open channels at the electrode tip in darkness.

The records at the top of Fig. 4 illustrate light responses from such an experiment. The trace labelled 'cell' was recorded from the inner segment with the suction electrode, while the trace labelled 'patch' was recorded simultaneously by a loose-patch electrode with an orifice 2·5 μm in diameter. The responses had similar waveforms. The response amplitudes were similar because the zero divalent Ringer solution in the patch electrode scaled up the loose-patch current, while the suction electrode recorded only a small fraction of the whole-cell current because little of the inner segment was drawn in. Similar, but smaller, loose-patch responses were observed using pipettes with an orifice 0·65 μm in diameter. For the recordings of Fig. 4 the corrected loose-patch current was 13·5 pA and the estimated whole-cell current was 54 pA (details in legend). The ratio of the currents was 0·25 for these responses and 0·19 averaged over all twenty-two trials on the cell. The average ratio for two other cells tested with a 2·5 μm loose-patch pipette was also near 0·2. Typically the corrected loose-patch current was about one-third the corrected whole-cell current recorded in the absence of the loose-patch electrode.

Figure 5*A* shows how loose-patch currents from three cells varied with circumferential position on the outer segment. The pipette's orifice was 2·5 μm, and current amplitudes are expressed relative to the mean amplitude from the cell. There is considerable scatter in the points, but sizeable responses were recorded at each position. There was no indication of a circumferential pattern such as a single longitudinal 'stripe' of open channels, nor of any periodic pattern with a scale larger than 2·5 μm. The scatter may reflect variations in patch area and/or perturbations in cyclic GMP induced by the loose-patch pipette (see Methods).

Figure 5*B* shows how loose-patch currents from two cells varied with longitudinal position on the outer segment. Again there was scatter in the amplitudes, but sizeable responses were obtained at each position and there was no indication of a systematic trend. These results are consistent with Baylor *et al.*'s (1979) finding that the dark current entering a unit length of the outer segment was the same at all longitudinal positions.

Do the amplitude variations in Fig. 5 arise from channel clusters somewhat smaller than the pipette diameter of 2·5 μm? Figure 6 compares distributions of current amplitude measured with 2·5 or 0·65 μm resolution. The distribution on the left is from all measurements at different positions on three cells with the larger pipette. The distribution on the right was obtained from three different cells with the smaller pipette, which was moved to various circumferential and longitudinal positions on the outer segments. As expected the smaller pipette measured smaller currents. The similar widths of the distributions argue against the existence of channel clusters larger than about 0·5 μm diameter.

These measurements indicate that open channels were present at approximately

uniform density around the circumference and along the length of the outer segment. Now patch pipette-induced variations in the open probability would have increased the scatter in the local current amplitude distributions (see Methods). Therefore, on a micrometre scale, the variation in the true active channel density should not exceed

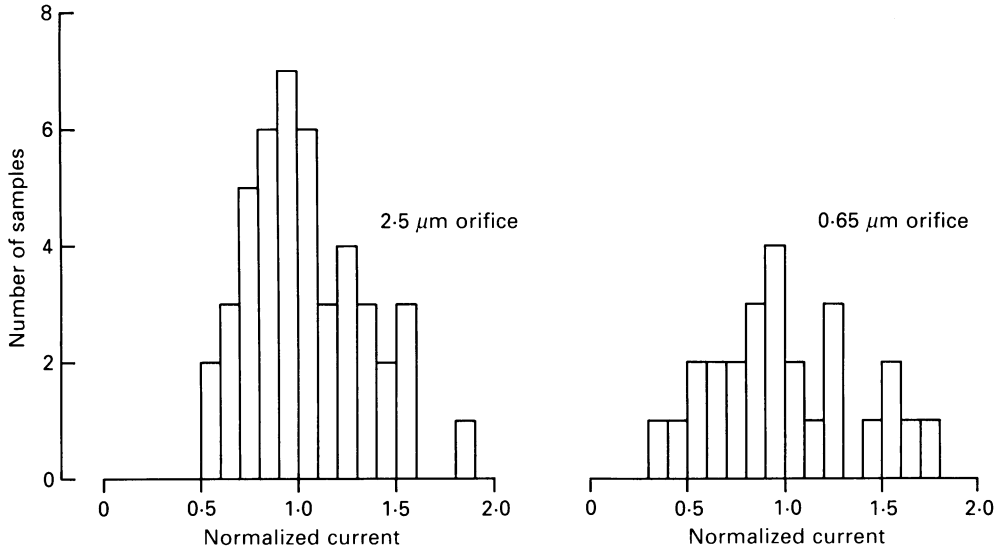

Fig. 6. Spread of photocurrent amplitudes at different positions on the outer segment, recorded with loose-patch electrodes, orifice 2·5 or 0·65 μm diameter. Each distribution based on results from three cells. Loose-patch current amplitudes from each cell are expressed relative to the mean amplitude from that cell. The distribution on the left is from the results plotted in Fig. 5; $n = 45$. For the distribution on the right the mean current amplitudes were 2·3, 1·4 and 2·6 pA; $n = 26$.

that of the distributions in Fig. 6, or about $\pm 50\%$. Since the excised patches usually had areas of at least 10 μm^2, it appears that a non-random spatial distribution of active channels cannot explain the widely varying active channel densities observed in excised patches.

Active channel density in patches excised from whole rods

Isolated outer segments from bleached rods cannot transduce and their metabolic condition is uncertain. Therefore we examined the active channel density in patches from dark-adapted, transducing rods. The inner segment of an isolated rod was drawn into a suction electrode and the response to a saturating flash was recorded. A patch was then excised from the outer segment and the density of active channels in the patch was measured. The distribution of channel density from sixteen experiments is shown by the histogram labelled 'dark cells' in Fig. 3. Again the measured density varied over a surprising range: 1·12–200 μm^{-2}, with a mean of 60 μm^{-2}. From the measured amplitude of the light response and the fraction of inner segment in the suction electrode the saturating response amplitudes for the cells were estimated as 45 ± 20 pA (mean $\pm$ standard deviation).

Patches excised from whole bleached cells judged by their appearance to be in good

condition gave the distribution labelled 'light cells' in Fig. 3. Except for one very high density of 641 μm^{-2}, this distribution is similar to that of 'dark cells'. The mean density was 96 μm^{-2} for all twenty bleached cells and 67 μm^{-2} when the single high density was excluded. These experiments, therefore, gave no evidence that the state of dark or light adaptation influenced the active channel density.

Many of the active channel densities in patches excised from dark-adapted transducing rods seem too low to be physiological. Corrected local dark currents of at least 15 pA were usually obtained in loose-patch recordings from a membrane area near 5 μm^2 (2·5 μm orifice). Assuming that the single-channel current was 0·8 pA at the dark potential (Matthews & Watanabe, 1987), the local current implies that 3·8 channels were open per square micrometre. Open channels represent only a small fraction of the total however. For example, the measured dark current of a transducing rod increases by up to 50 times when a hydrolysis-resistant analogue of cyclic GMP is infused into it (Zimmerman, Yamanaka, Eckstein, Baylor & Stryer, 1985). Since the series resistance as well as ionic accumulation will limit the current increase, the fraction of channels open in darkness cannot be much more than 0·01–0·02 (reviewed in Yau & Baylor, 1989). This implies at least 200–400 active channels per μm^2. Yet, many of the densities in patches excised from transducing rods were far below this. Nine of the sixteen patches had densities below 40 μm^{-2}, and four had densities below 10 μm^{-2}. This large discrepancy, as well as the wide range of densities in the excised patches, suggests that obtaining a patch lowered the density of active channels in the membrane.

Time course of patch current after excision

The density of active channels might be lowered by sealing the electrode on the outer segment or excising the patch. In an attempt to observe the time course of such an effect of excision we recorded the patch current while excisions were made from bleached whole cells into a solution containing 500 μM-cyclic GMP. Within about 1 s of excision the patch current jumped to a new level; during the lag cyclic GMP from the bulk solution diffused to the cytoplasmic surface of the channels. Washing with control solution indicated that most of the new current was cyclic GMP activated. After small changes in the current over the next 30 s or so the cyclic GMP-activated current was usually quite stable for the life of the patch. This indicates that channel density did not fall because channels were adsorbed at the rim of the seal nor because of slow denaturation of channels, both of which should have continued as long as the patch survived. In the first 30 s after excision, small changes in the current sometimes occurred, but there was no indication of a time-dependent channel shut-off. In four cases the final active channel density had low values less than 20 μm^{-2}, so that the active density must have been lowered. Yet only twice did the current sag at all within the first half-minute in these experiments, and the small sags (10 and 30% respectively) were accompanied by a decrease in the membrane area, indicated by a decrease in the capacitive transients. Therefore the small decrease in patch area apparently occurred without an appreciable change in active channel density. In nine experiments the final channel density was relatively high, > 100 μm^{-2}. Typically the current rose rapidly to a plateau, then crept upward over the next 10–30 s by about 10%.

The stability of the patch current after excision suggests that the active channel density was lowered by formation of the seal and/or by a nearly instantaneous effect of excision.

Effect of Ca^{2+} concentration on channel density

Figure 7 shows channel density distributions of patches excised from light-adapted whole cells bathed in Ringer II solution or exposed to zero-Ca^{2+} solution (sodium,

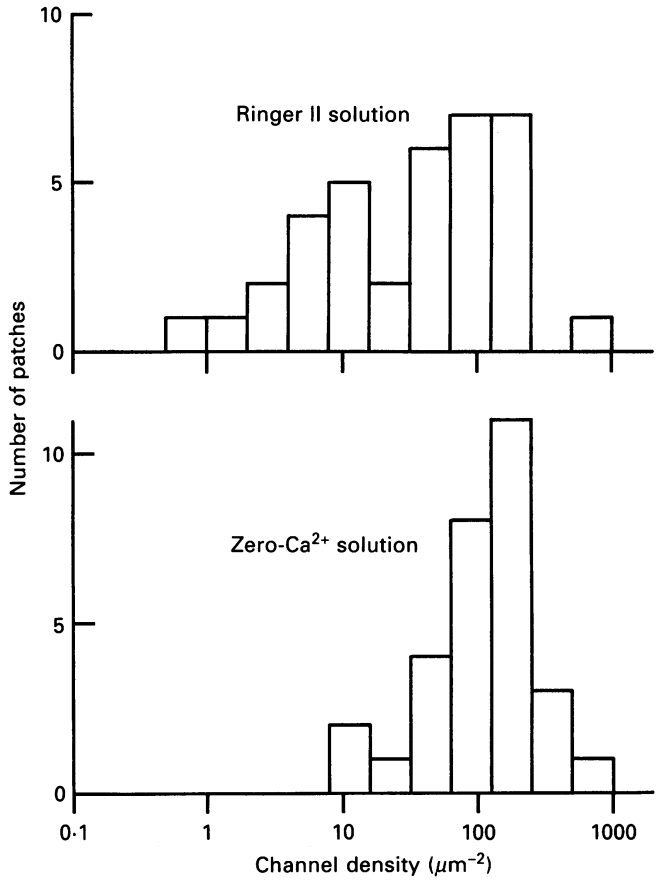

Fig. 7. Active channel densities from whole rods bathed in Ringer II or zero-Ca^{2+} solution containing 0 or 100 μM-Mg^{2+} (sodium, zero divalent solution or excising solution II, Table 1). For Ringer II solution the active channel density was 80 ± 117 μm^{-2} (mean $\pm$ standard deviation, $n = 36$) and the mean patch area was 11·5 μm^2. For zero-Ca^{2+} solution the active channel density was 152 ± 128 μm^{-2} (mean $\pm$ standard deviation, $n = 30$) and the mean patch area was 8·2 μm^2. Ringer II solution results are the sum of the dark- and light-adapted cell distributions in Fig. 3. In the zero-Ca^{2+} experiments the seal was obtained in Ringer II solution and the cell was then exposed to the zero-Ca^{2+} solution for about 2 min before excising. Rods in the zero-Ca^{2+} experiments were light adapted.

zero divalent solution or excising solution II) for about 2 min after sealing in Ringer II solution. The normal Ringer solution results are the sum of the dark and light distributions in Fig. 3, which did not appear to be systematically different. In the

histograms, density is plotted logarithmically because a linear scale did not show the wide range of densities in the lowest bin. The distributions overlapped, but the very low densities in the Ringer solution distribution were absent in the zero-Ca^{2+} distribution. The density in zero Ca^{2+} was 152 ± 128 μm^{-2} (mean $\pm$ standard deviation), while the density in normal Ringer solution was 80 ± 117 μm^{-2}. Under the null hypothesis, the difference between the population means will be normally distributed with a standard deviation $\bar{\sigma}$ given by

$$\bar{\sigma} = \sqrt{\left(\frac{\sigma_1^2}{n_1} + \frac{\sigma_2^2}{n_2}\right)}, \quad (2)$$

where σ_1 and σ_2 are the standard deviations and n_1 and n_2 are the sample sizes of the populations. The observed difference in the means exceeds 3·5 $\bar{\sigma}$, and therefore the null hypothesis is rejected at $P < 0{\cdot}0002$ (Brown & Hollander, 1977, p. 118).

Evidence suggesting that the difference in the two distributions depended on an effect of Ca^{2+} concentration rather than the total concentration of divalent cations was provided by comparing densities in patches excised from rods exposed to 100 μM-Mg^{2+}, 10 μM-Ca^{2+} Ringer solution, or to the same solution without Ca^{2+}, after the seal was formed in Ringer II solution. For seven patches excised in excising solution I, which contained 10 μM-Ca^{2+}, the density was $54{\cdot}2 \pm 75{\cdot}8$ μm^{-2} (mean $\pm$ standard deviation). This is similar to the density from the larger group of patches excised into Ringer solution. In comparison, eight patches excised in excising solution II, which lacked Ca^{2+}, gave densities of 137 ± 104 μm^{-2} (mean $\pm$ S.D.). The latter patches are members of the larger population illustrated at the bottom of Fig. 7. Using the test above for the significance of the difference between the means, the null hypothesis can be rejected at the $P < 0{\cdot}05$ level.

These results suggest that the concentration of Ca^{2+} ions in the bathing solution may influence the measured density of active channels.

DISCUSSION

Absolute channel density

In excised patches three active channel densities over 600 μm^{-2} were observed. These values appear to represent a lower limit for the true average density of channels in the surface membrane, not samples from local 'hot spots'. The evidence for this interpretation is that the areas of the three patches of high density ranged from 3 to 8 μm^2, and two other patches with densities over 500 μm^{-2} had areas greater than 18 μm^2; no such hot spots were observed in high-resolution loose-patch recording. The simplest interpretation is that copies of the channel protein are present at an average density of at least 650 μm^{-2}, and that the density of active channels, measured in excised patches, is usually lower.

Spatial arrangement of channels

Loose-patch recordings showed that open channels were present at fairly constant density along the length and around the circumference of the outer segment. Assuming that channels at all locations have a similar sensitivity to cyclic GMP, this implies that the distribution of all active channels (closed plus open) is like that

of open channels. A constant longitudinal channel density is required for efficient single-photon detection because a photon may be absorbed at any longitudinal position and the response to a photon is highly localized (Lamb, McNaughton & Yau, 1981). The constancy of open channel density around the circumference of the rod is consistent with results of Caretta & Saibil (1989), who used fluorescence microscopy to observe the binding of fluorescein-labelled cyclic GMP to isolated rod outer segments. Their pictures suggest a roughly constant density of label around the circumference of most of the outer segment except at the base, where longitudinal bands of higher density were interpreted as channels on calycal processes from the inner segment.

In some bovine rod preparations the cyclic GMP-activated channel co-purifies with a protein related to spectrin (Molday *et al.* 1990), which has been localized to disc rims (Wong & Molday, 1986). Since there are about thirty discs per micrometre length, a periodicity associated with anchoring to the discs would be far below the resolution of our measurements.

Variable channel densities in excised patches: physical artifact or channel regulation?

Active channel densities varied widely between excised patches under all conditions, and typical densities were far below the high values of over 600 μm^{-2}. Since the low values and the variability cannot be explained by a non-random spatial arrangement, it appears the powerful mechanism(s) can lower the density of active channels. The existence of such an effect may bring into question the assumption that channels in excised patches are functionally identical to channels in transducing cells. Several mechanisms, acting multiplicatively, may have contributed to the very wide range of densities that were observed. What might these mechanisms be?

One possibility is that patch excision lowered the active channel density by a physical effect. Stretch on the patch might irreversibly disrupt channels, or cause mixing between the surface membrane and disc membranes, which lack channels (Bauer, 1988; Cook *et al.* 1989; Caretta & Saibil, 1989). The lack of correlation between patch area and active channel density, however, offers no support for these mechanisms. Thus for patches of large area more suction was required to obtain the seal, and the seal formed more slowly. This might have given lower densities. There was also no obvious correlation between measured channel density and the degree or duration of indenting the outer segment with the pipette prior to applying suction. Even if disc lipids entered the surface membrane during seal formation or excision, it seems unlikely that the effect would be large enough to lower the channel density by over two orders of magnitude. The stability of the cyclic GMP-activated current after excision rules out progressive adsorption of channels to the glass at the seal, poisoning of channels by ions from the pipette glass or solution, or progressive denaturation of channels.

A second possibility is that the channel's ability to respond to cyclic GMP is subject to enzymatic regulation, and that disturbing the cell with the patch electrode perturbs this regulatory mechanism. Suppose that the outer segment contains enzymes that convert the channel between a form that responds to cyclic GMP and a form that does not. Obtaining a patch might bias the system to turn channels off and produce low active channel densities. Two observations seem consistent with this notion: (1) patches from whole cells bathed in solutions containing or lacking Ca^{2+}

exhibited different density distributions (Fig. 7); (2) patches from isolated outer segments, which were presumably depleted of high-energy phosphate compounds, had a higher mean channel density than patches from whole cells (Fig. 3). Perhaps also consistent with this interpretation, Matthews & Watanabe (1987) reported that some cell-attached patches on transducing rods failed to show single-channel activity until the external Ca^{2+} concentration was lowered.

This work was supported by grant 1 R01 EY01543 from the National Eye Institute, USPHS, an award from the Retina Research foundation, and fellowships from the Bank of America-Giannini Foundation (J.K.), the Stanford Medical Scholars Program (D.L.) and National Medical Fellowships (D.L.). We thank Robert Schneeveis for excellent technical assistance, Professor Lubert Stryer for useful suggestions, and Drs Richard Aldrich, Leon Lagnado and Markus Meister for comments on the manuscript.

REFERENCES

BAUER, P. J. (1988). Evidence for two functionally different membrane fractions in bovine retinal rod outer segments. *Journal of Physiology* **401**, 309–327.

BAYLOR, D. A., LAMB, T. D. & YAU, K.-W. (1979). The membrane current of single rod outer segments. *Journal of Physiology* **288**, 589–611.

BAYLOR, D. A. & NUNN, B. J. (1986). Electrical properties of the light-sensitive conductance of rods of the salamander *Ambystoma tigrinum*. *Journal of Physiology* **371**, 115–145.

BODOIA, R. D. & DETWILER, P. B. (1985). Patch-clamp recordings of the light-sensitive dark noise in retinal rods from the lizard and frog. *Journal of Physiology* **367**, 183–216.

BROWN, B. W. & HOLLANDER, M. (1977). *Statistics: a Biomedical Introduction*. John Wiley and Sons, New York.

CARETTA, A. & SAIBIL, H. (1989). Visualization of cyclic nucleotide binding sites in the vertebrate retina by fluorescence microscopy. *Journal of Cell Biology* **108**, 1517–1522.

COOK, N. J., MOLDAY, L. L., REID, D., KAUPP, U. B. & MOLDAY, R. S. (1989). The cGMP-gated channel of bovine rod photoreceptors is localized exclusively in the plasma membrane. *Journal of Biological Chemistry* **284**, 6996–6999.

FALK, G. & FATT, P. (1968). Passive electrical properties of rod outer segments. *Journal of Physiology* **198**, 627–646.

GRAY, P. & ATTWELL, D. (1985). Kinetics of light-sensitive channels in vertebrate photoreceptors. *Proceedings of the Royal Society* B **223**, 379–388.

HAYNES, L. W., KAY, A. R. & YAU, K.-W. (1986). Single cyclic GMP-activated channel activity in excised patches of rod outer segment membrane. *Nature* **321**, 66–70.

HILLE, B. (1984). *Ionic Channels of Excitable Cells*. Sinauer, Sunderland, MA, USA.

KARPEN, J. W., LONEY, D. A. & BAYLOR, D. A. (1990). Density and spatial distribution of cGMP-activated channels in the surface membrane of retinal rods. *Biophysical Journal* **57**, 372a.

LAMB, T. D., MCNAUGHTON, P. A. & YAU, K.-W. (1981). Spatial spread of activation and background desensitization in toad rod outer segments. *Journal of Physiology* **403**, 473–494.

LONEY, D. A., KARPEN, J. W. & BAYLOR, D. A. (1989). Density of cGMP-activated channels varies by three orders of magnitude in surface membrane of salamander rod outer segments. *Investigative Ophthalmology and Visual Science* **30**, 61.

MCNAUGHTON, P. A. (1990). Light response of vertebrate photoreceptors. *Physiological Reviews* **70**, 847–883.

MATTHEWS, G. & WATANABE, S.-I. (1987). Properties of ion channels closed by light and opened by guanosine 3′,5′-cyclic monophosphate in toad retinal rods. *Journal of Physiology* **389**, 691–716.

MATTHEWS, G. & WATANABE, S.-I. (1988). Activation of single ion channels from toad retinal rod inner segments by cyclic GMP: concentration dependence. *Journal of Physiology* **403**, 389–405.

MOLDAY, L. L., COOK, N. J., KAUPP, U. B. & MOLDAY, R. S. (1990). The cGMP-gated channel of bovine rod photoreceptor cells is associated with a 240-kDa protein exhibiting immunochemical cross-reactivity with spectrin. *Journal of Biological Chemistry* **265**, 18690–18695.

PENN, R. D. & HAGINS, W. A. (1972). Kinetics of the photocurrent of retinal rods. *Biophysical Journal* **12**, 1073–1094.

SAKMANN, B. & NEHER, E. (1983). Geometric parameters of pipettes and membrane patches. In *Single Channel Recording*, ed. SAKMANN, B. & NEHER, E., pp. 37–51. Plenum Press, New York.

TAYLOR, W. R. & BAYLOR, D. A. (1990). Kinetics of single cGMP activated channels from rod outer segments. *Investigative Ophthalmology and Visual Science* **31**, 176a.

WATANABE, S.-I & MATTHEWS, G. (1988). Regional distribution of cGMP-activated ion channels in the plasma membrane of the rod photoreceptor. *Journal of Neuroscience* **8** (7), 2334–2337.

WONG, W. & MOLDAY, R. S. (1986). A spectrin-like protein in retinal rod outer segments. *Biochemistry* **25**, 6294–6300.

YAU, K.-W. & BAYLOR, D. A. (1989). Cyclic GMP-activated conductance of retinal photoreceptor cells. *Annual Review of Neuroscience* **12**, 289–327.

YAU, K.-W., HAYNES, L. W. & NAKATANI, K. (1986). Roles of calcium and cyclic GMP in visual transduction. In *Membrane Control of Cellular Activity*, ed. LUTTGAU, H. CH., pp. 343–366. Gustav Fischer, Stuttgart.

ZIMMERMAN, A. L. & BAYLOR, D. A. (1986). Cyclic GMP-sensitive conductance of retinal rods consists of aqueous pores. *Nature* **321**, 70–72.

ZIMMERMAN, A. L., KARPEN, J. W. & BAYLOR, D. A. (1988). Hindered diffusion in excised membrane patches from retinal rod outer segments. *Biophysical Journal* **54**, 351–355.

ZIMMERMAN, A. L., YAMANAKA, G., ECKSTEIN, F., BAYLOR, D. A. & STRYER, L. (1985). Interaction of hydrolysis-resistant analogs of cyclic GMP with the phosphodiesterase and light-sensitive channel of retinal rod outer segments. *Proceedings of the National Academy of Sciences of the USA* **82**, 8813–8817.